Trinity University

Digital Commons @ Trinity

Engineering Senior Design Reports

Engineering Science Department

5-6-2020

HaptX Team Final Project Report

Lydia Matteson
Trinity University

Morgan Jones
Trinity University

Sam Hinojosa
Trinity University

Interoffice Memorandum

TO: Dr. Emma Treadway, Assistant Professor of Engineering Science, Trinity University
Dr. Darin George, Senior Design Administrator

FROM: The HaptX Team: Lydia Matteson, Morgan Jones, Sam Hinojosa

SUBJECT: Final Project Report

DATE: May 6, 2020

CC: N/A

NOTE: To help aid the reader with understanding how the design works, we have included a short video of it being operated by the user. This may help with visualization of the motion of the device while reading through section 1.2. However, it may also help conceptualize what a haptic device should look like in the Introduction.

Executive Summary

A traditional haptic device utilizes motors to impose feedback motion constraints on a user interacting with it. However, primary concerns with human-robot interaction include safety, stability, and ease of manufacturing. It is therefore desired to develop a passive haptic device that users can interact with by moving the system along constrained single degree of freedom (SDOF) paths while restricting motion in other directions. The goal of the project is to develop a planar passive haptic system that can restrict motion paths while allowing only the prescribed SDOF paths.

The device is required to have at least six SDOF paths and force resistance capable of blocking the user when they deviate away from an SDOF path and preventing them from damaging the device. Additionally, the minimum angle between adjacent SDOF paths must be less than 90 degrees.

The design that we chose was a system of six linkages connected by brakes at each joint. These brakes are pneumatically powered and turn on and off to hold and release the motion of the linkages. Rotary encoders are mounted at the bottom of the brakes to track the relative position of the joints and the handle that is moved by the user. The primary requirements were that the system had at least 6 SDOF paths and could resist a maximum torque of 11Nm, produced by a user at the handle.

To test that the device matched the characteristics and requirements that it was designed, the assembled prototype was subject to many tests, as well as virtual simulations. Some requirements and constraints were achieved simply by nature of the design. For example, the six SDOF paths are inherently included in the design by the addition of 6 brakes, and therefore it does not need to be confirmed through testing. However, some tests were performed to test the functionality, including both angle measurement and force testing for one linkage, as well as the full system. In addition, MATLAB simulations verified the angle change between the different degrees of freedom paths. Each of these tests verified different parts of the requirements. All of these tests were successful.

There are no major modifications that need to be made to the device moving forward. All requirements for design have been met. However, there are modifications that should be made to increase the ability and accuracy of the device. Currently there is too much slack in the joints that will not only affect force, but position measurements as well. This issue should be address to improve the device.

1. Introduction

Haptic systems for gaming or training simulations often require motion to be constrained to render virtual environments.These systems can impose virtual motion constraints, which constrain users to follow single-degree-of-freedom (SDOF) paths in an open space. One example is using a haptic controller for a virtual maze game, which involves virtual boundaries for the walls of the maze. Other examples include creating paths to guide a surgeon to make the appropriate operation in a simulated clinical test. In applications such as these, safety and stability are essential features.

Active haptic systems are used quite frequently for applications of virtual environments, and are typically actuated with motors, which are used to restrict the motion of the user. However, safety concerns arise when these motor-actuated devices are utilized in larger workspaces that cover large or whole-body movements. However, passive devices do not use power to create motion, which allows users to move the robot using only the forces from their hand, arm, or body. Therefore, these devices show potential as safer devices than active haptic designs for larger workspaces, but can still impose paths by passively constraining the user's motions.

Several of Dr. Treadway's studies proposed utilizing a digital hydraulic system to passively restrict motion to SDOF paths [1]. Additionally, studies by Reed and Book developed a passive device consisting of linkages and brakes [2]. However, both of these components may not suffice for a table-top haptic device, and consequently, do not completely satisfy requirements for the system because the digital hydraulic system was used for an exoskeleton and the linkage system consisted of high-cost-variable-brake resistance. Our group was therefore tasked with researching, designing, and implementing an appropriate design for a planar tabletop passive haptic device so that the sponsor can then study various controllers to change device paths.

1.1 Project Requirements and Constraints

In the designing of our project, there were many objectives that needed to be met, and many constraints and standards that were to be followed. The main goal of the project were the required six SDOF paths that were to be available at any position of the handle.

1.1.1 Constraints for the project:

1.1.1.1 Passive Haptic Device - It is crucial that our design must be functionally passive, meaning that the system cannot “create” trajectory motion for the user with actuators, but only block them from moving outside the specified path.

1.1.1.2 Discretely Variable SDOF System - In the context of haptic devices, variable path constraints can be either discrete or continuous. Discretely variable devices can constrain motion to one of a finite number of directions, along SDOF paths, each of which is instantaneously available. In contrast, a continuously variable device can constrain paths in any direction, but must smoothly steer to each direction. An example of a passive continuous SDOF haptic device is the cobot, which changes directions by steering with rolling contacts. Therefore, we plan to focus our designs on discretely variable SDOF systems for the purpose of the research.

1.1.1.3 Trajectory Angle - The angle between adjacent trajectories needs to be less than 90 degrees over a size of 12in x 5in.This is an important constraint that prevents the user from moving opposite the intended direction when the device switchesSDOF paths.

1.1.2 Applicable Codes and Standards:

1.1.2.1 Federal Guidelines from the Institutional Review Board - Dr. Treadway’s research for haptic devices have been approved as an “exempt” project, meaning that our project must abide by the following federal guidelines provided by the Institutional Review Board [3]:

> "(ii) For the purpose of this provision, benign behavioral interventions are brief in duration, harmless, painless, not physically invasive, not likely to have a significant adverse lasting impact on the subjects, and the investigator has no reason to think the subjects will find the interventions offensive or embarrassing. Provided all such criteria are met, examples of such benign behavioral interventions would include having the subjects play an online game, having them solve puzzles under various noise conditions, or having them decide how to allocate a nominal amount of received cash between themselves and someone else."

1.1.2.2 ISO 10218-Robot system/cell - The International Organization for Standardization (ISO) consists of the following appropriate clauses for our design [4]:

5.10.2 No robot motion when the operator is in a collaborative work space

5.10.3 Robot motion is only controlled through the direct input of the operator

5.10.4 Robot motion is only controlled when the separation distance is above the minimum separation distance

5.10.5 In contact events, the robot can impart limited static and dynamics forces

Note that because the system is passive, we are already assuming that clause 5.10.3 already suffices, because the device is inherently incapable of moving without the supplied motion from the user.

1.1.3. Functional Requirements:

The haptic device must have at least 6 SDOF paths and the user should be able to move freely when following the preset path. Additionally, the device must withstand 25N in the direction perpendicular to the SDOF path, which translates to an estimated torque of 11Nm for the worst-case. These values were discussed and agreed upon as acceptable criteria by our sponsor and advisor Dr. Treadway. Additionally, the system should not be damaged by the user interacting with it. Lastly, the position of the handle must be measured.

1.1.4. Non-functional Requirements:

It is important that the device is to be used on a table, therefore it shall not be larger than the table in Dr. Treadway's laboratory. Additionally, the size of the workspace should be roughly a 12in x 5in area.

1.1.5. Interface Requirements:

The device should generally be user friendly, which is specified by the handle being an appropriate size for the average adult, and the device having minimal friction, inertia, and vibrations when the user moves it. It must also ensure that the user operating it does not experience any pinching points for any parts of the body.

1.2 Brief Summary of Design

We designed a system that makes rotary SDOF paths. The handle of the system was attached to a set of linkages that pivot and rotate at each joint. An individual joint with its pneumatic cylinder and encoder can be seen in Figure 1 below. Pneumatic brakes were installed at each of the six joints to stop the relative motion caused by a user. Rotary encoders were also installed onto the joints to measure the relative motion caused by a user moving the handle, which satisfies the requirements of measuring the handle position. The brakes satisfy the requirement of multiple SDOF paths, and their effective bore-sizes were selected to satisfy the force requirement. The full design with all six joints is shown in Figure 2 and the assembled device is shown in Figure 3.

1.2.1 How the Device Works

When the system is in operation, five out of the six cylinders use solenoid valves to extend the piston head, and the attached brake disk pushes down onto the brake disk (refer to Figure 1), which in turn locks the rotational motion of the joint. The last cylinder, which can be any of joints 1-6, remains retracted, allowing rotational motion about that joint. A user can then rotate the handle about the pivot of that open joint, which creates an SDOF path. The user can open and close any cylinders, to make different SDOF paths, but exactly five of the cylinders must be closed while one must remain open.

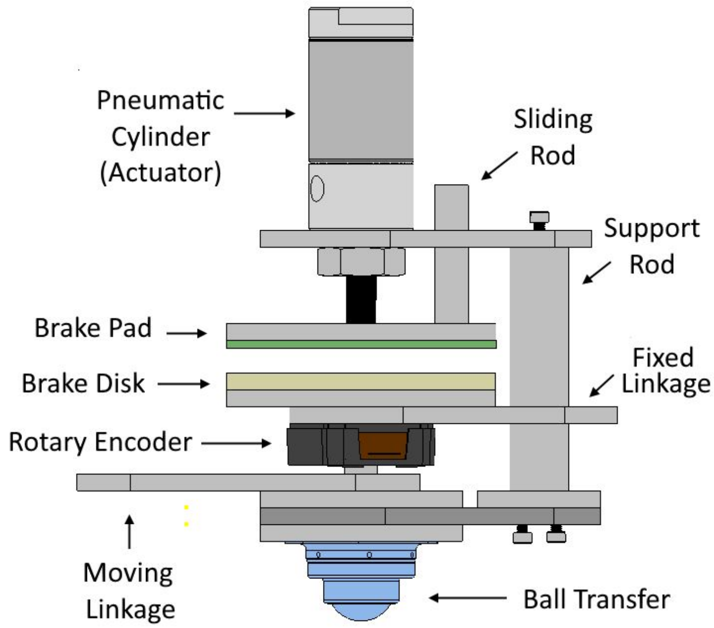

Figure 1. Design of the single joint for the haptic device.

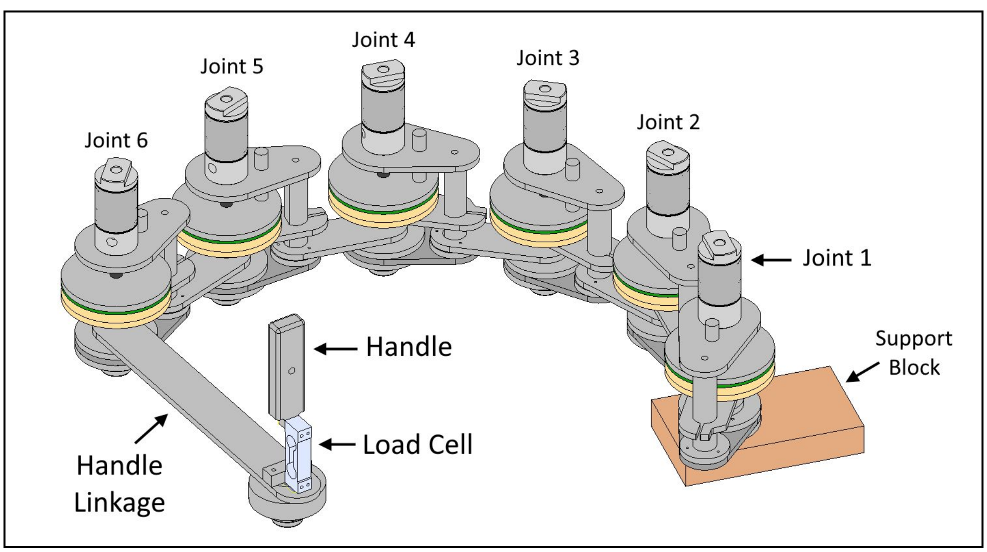

Figure 2. Full system assembly of the haptic device. Note that all six single joints are connected to each other.

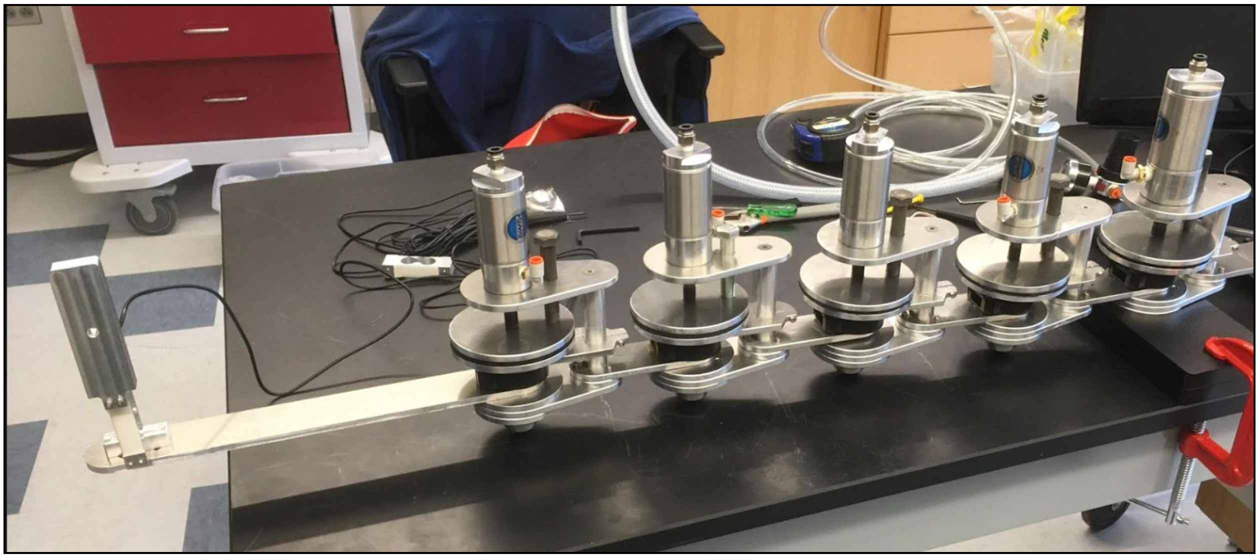

Figure 3. Physical prototype machined and assembled by Ryan Hodge. Note that only five joints are shown in the figure because of limited time for the project and availability of the staff to help during remote learning. This does not affect our testing for the force and torque requirement, which is described in section 3.2.2.

2. Overview of the Final Design

The primary design components of the haptic device include the pneumatic actuators, brake disks, data acquisition (DAQ) measurements, and single degree of freedom (SDOF) paths.

2.1 Geometry of Haptic Device and Theory of Maximum Torque on Joints.

Figure 4 illustrates the geometry of the haptic device. The considerations for the geometry and positioning of the system was made primarily to satisfy both the force and angle requirements. Therefore we designed the nominal angle between joints to be 160 degrees and the angle between the handle to be 75 degrees. The resulting maximum distance from the handle was from joint 6, and was calculated to be 17.4in (0.44m), and we used this value to compute the maximum torque on the joint. The estimated torque, as well as the torques on the other joints, were shown in Table 1.

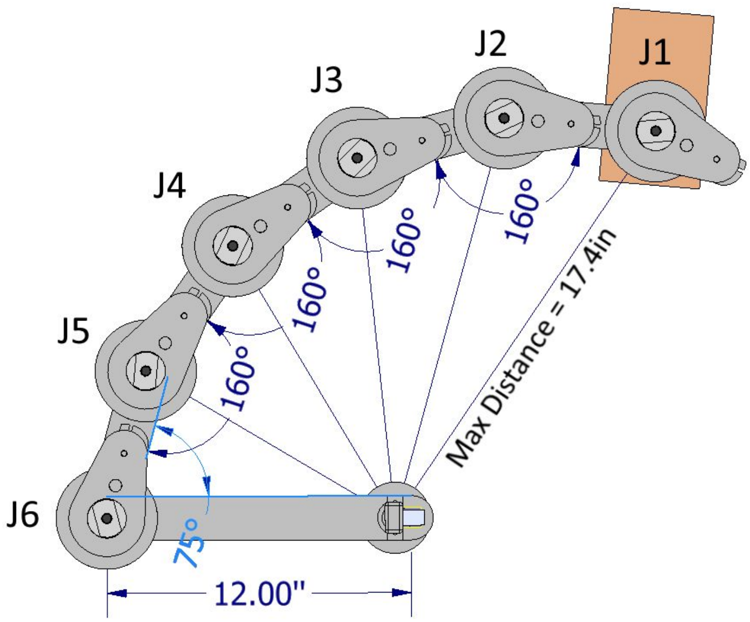

Figure 4. Full extension (all joints are extended to 160 degrees and the handle to 75 degrees) of the complete assembly. The maximum distance from the handle is shown to be from joint 1.

2.2 Actuators

Designing these pneumatic brakes from scratch was a major design change since the preliminary design report last semester, necessitated by budget constraints and bad information from a sales representative. Thus, the following sections describe the theoretical calculations made to ensure that the design would meet the right requirements and fit within budget. The pneumatic cylinder at the top of each joint of the device pushes onto the brake disk and uses friction force when engaged to counteract any force applied by a user that would tend to cause rotation about that joint. The force produced by the cylinder comes from an air supply of ~70 psi (gauge). The size of brake disks, as well as the material were designed to produce enough frictional force (when in contact with the actuator) to resist the maximum user's pulling/pushing force of 25N and a torque of 11Nm. An electrical solenoid valve was also required to extend and retract each cylinder.

2.2.1 Design and Theory of Torque Resistance

The calculation of torque resistance due to the friction is based on the equation of static friction, as shown in Eq. 1.

$$F = u_s F_{Load} \quad \textbf{(1)}$$

The cylinder head is modelled as a solid circular area, A with radius, r, which provides a force, F onto the contact disk. This model is shown in Figure 5. We sum up the individual moments over the contact disk using Equation 2 [5] (p is the normal force pressure at the differential point and r is the distance from that point to the center of rotation):

$$M = \int_A dM = \int_A u_s * p * r * dA \quad \textbf{(2)}$$

In the reference of [5], they use a contact area of disk with an inner radius Ri, however we can arrive at Eq. 3 by setting the inner radius, Ri to 0, which represents a solid contact disk:

$$M = \tfrac{2}{3} u_s * F_{Load} * R_0 \quad \textbf{(3)}$$

Using Equation 3, we chose the appropriate piston bore-sizes that would supply enough force to resist the max torque caused by a user's hand on the handle described in Table 1. Other important considerations in selecting the actuator size were the weight of the cylinder, and its cost, as well as the cost of the corresponding valves. We chose a double-acting pneumatic cylinder over a single acting cylinder to obtain the maximum possible normal force from the air supply. A bore size of 1.75in for the cylinders were selected for joints 1 and 2 (refer to Figure 4) and a bore size of 1.5in were chosen for joints 3-6.

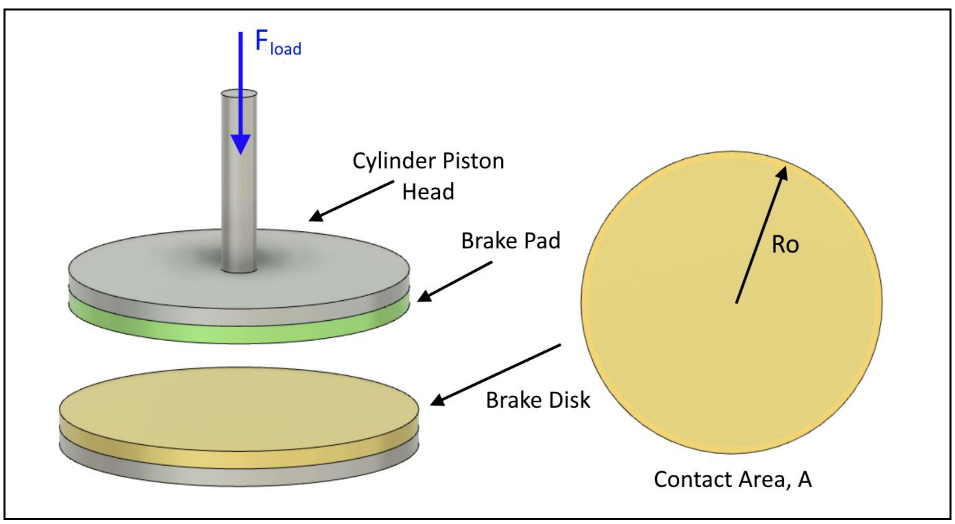

Figure 5. Schematic representation of the cylinder head (brake pad in Fig. 1) onto the contact disk (brake disk in Fig 1)

2.3 Physical Structure

The first physical prototype of the brake that we machined can be seen in Figure 6 below. After building this prototype we realized that a few changes could be made to improve the overall function of the brake in addition to simplify some of the machining for the next five brakes.

Figure 6. Assembled brake with the 3D printed shaft

After conducting some preliminary testing on the first prototype it was clear that the 3D printed shaft that we were using to save time could only withstand minimal torque so it needed to be replaced with a steel shaft. In addition to replacing the shaft we also discovered that the keyway in the original design (that held the top disc in place which the top arrow is referring to in Figure 7) was not practical to machine as it needs to be hammered into place.

In addition, for the first prototype that can be seen in Figure 6, we pinned the linkage to avoid damaging the encoder that would be located directly below it (illustrated in Figure 1). However, it is very challenging to pin the linkage into place as the vertical location of the linkage must be very precise and cannot be adjusted after it is hammered into place. To adjust for this issue we decided to alter the shape of one end on the linkage to create a clamp that can be easily adjusted and still prevent it from resting on the encoder (can be seen in Figure 7).

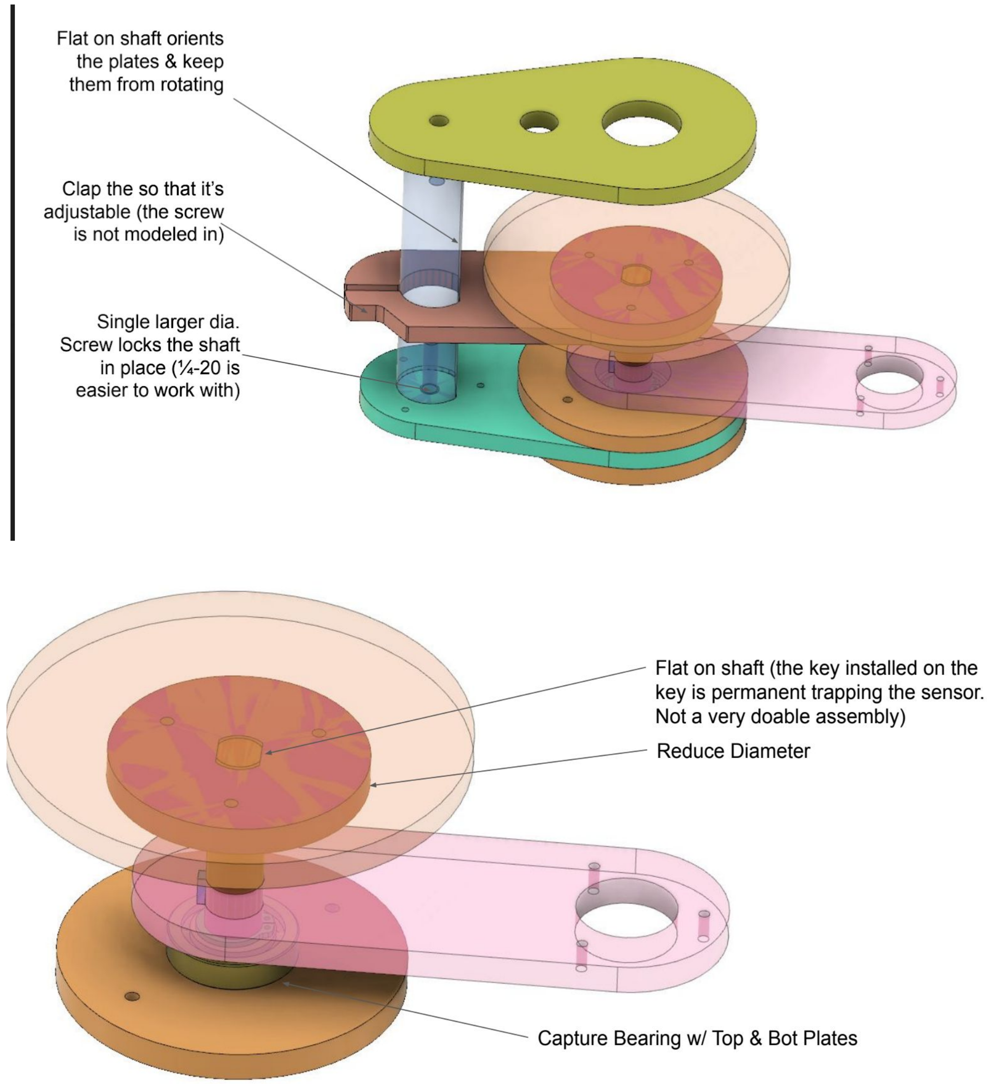

Figure 7. Changes made to brake design after testing the first prototype

In addition, we also decided that there was no reason for the large diameter of the disc above the fixed linkage so we reduced its size in the hope of not wasting materials. Also, we reduced the inner diameter of the bottom disc seen in Figure 7. The inner diameter of the disc was reduced to be smaller of the ball bearing located above it to reduce any vertical movement of the bearing. The full protype of the assembly of the updated brake design can be seen in Figure 3 and was machined and assembled by Mr. Hodge in the machine shop. In order to create the prototype he used the CNC machine to cut out all of the aluminum pieces from a CAD model we sent to him. Also, the bandsaw was used to cut the aluminum and steel rods and the drill press was used to add all the holes for the screw locations. In addition, some of the holes created by the drill press were tapped in order to create threads for the screws.

2.4 Position Sensors

Under each of the brake disks, there is a rotary encoder (E2 encoder from US Digital). The base of the encoder is attached to the fixed linkage, while the rotating disc of the encoder is attached to the rotating shaft. This encoder measures the angle of each brake that can be used to find the handle position. This is necessary to be able to track the movement of the user's arm.

2.4.1 Design and Theory of Handle Position

The theory used for the handle position relies on simple geometric principles. Applying the position of the handle on a workspace, its measurement is presented in terms of the X and Y directions. By evaluating the respective angles of each brake, you can find the final distance of the handle using geometry, in respect to the horizontal. The equations used to find the applied angles can be found in Table 2, and the equations used to analyze those angles for the position can be found in Table 3.

3. Design Evaluation

3.1 Force and Torque Resistance

To evaluate the maximum force and torque the prototype is able to withstand we conducted two tests. The first test focuses on finding the maximum torque a single brake is able to resist before slipping occurs while the second test determines that of the full assembly.

3.1.1 Single Joint Torque Testing

This test evaluated the maximum force and torque that a single joint with a 1.5 in bore cylinder can resist before slipping occurs.

Objectives

The team used a load cell to determine the maximum torque one brake can withstand before slipping occurs.

Design feature evaluated

The test evaluated the maximum torque a single joint can resist.

Test scope and key test conditions

A load cell was used to measure the force the brake is resisting when locking out motion. The load cell was positioned perpendicular to the constrained path as it can only measure force in one direction. The data was collected using MATLAB Simulink, from this data the torque was then calculated.

Instruments and/or test setups used

This testing required a load cell that was provided by Dr. Treadway and a new linkage and handle that can be seen in Figure 3. A force will be applied to the handle until the brake begins to slip. This data from the load cell will be collected using MATLAB Simulink and from that data we will be able to determine the maximum torque force the brake can withstand

Any assumptions involved in the testing

The main assumptions in this test is that the calibration plot of the same load cell would not change over time, and the force produced by the user is strictly tangential to the SDOF path.

Acceptance criteria

For our design the brake must be able to resist at least 7.62 Nm of torque for the 1.5in bore cylinder.

Test Results

The team conducted preliminary testing on the first prototype of the single joint with the 3D printed shaft that can be seen in Figure 6. We had purchased a steel keywayed shaft but the diameter of the shaft was slightly too large and needed to be lathed for the retaining rings. In the hope of moving forward with some testing of the first prototype to determine if it was functional we decided to conduct some testing with the 3D printed shaft. However, when presented with a minimal amount of torque the 3D printed shaft broke.

After the 3D printed shaft broke, Mr. Hodge assisted us with machining the brakes with the steel shaft which can be seen in Figure 3. With the update to the shaft we were able to conduct further force/torque testing. The results of this single joint testing can be seen in Figure 10 in Appendix C, which can be found in the Appendix C. Since the smaller cylinder with a bore size of 1.5in was tested we expected it to resist 7.62 Nm of torque. On the plot you can see that the brake was able to withstand the expected amount of torque before slipping occured, which is 7.62 Nm.

Evaluation

From the test results our design meets the acceptable criteria since a single joint with a 1.5in bore cylinder is able to resist 7.62 Nm of applied torque.

3.1.2 Full Assembly Force/Torque Testing

The test will demonstrate the overall force/torque resistance that the system can provide when someone tries to divert from the SDOF path.

Objectives

The design team will use a load cell to determine the maximum force the entire system of linkages and brakes.

Features evaluated

The test will evaluate the ability of the system to resist an applied force of 25 N and torque of 11Nm for the cylinder with a bore size of 1.75in .

Test Scope and Key Test Conditions

A load cell was positioned perpendicular to the desired path to read the maximum force the brake can withstand before slipping occurs. The data from the load cell was collected using MATLAB Simulink. Because we have only five joints in the full assembly, we re-positioned the system to get the correct moment arm from the handle to the base joint. This is shown in Figure 9 in Appendix C, and the measured length is 17in.

Instruments and/or Test Setups Used

This testing will use a load cell that is applied to a metal handle and mounting plate. The handle linkage will be from the furthest joint from where the system is mounted. Once calibrated and mounted to the appropriate moving linkage a force will be applied until slipping occurs.
The data from the load cell will be collected using MATLAB Simulink and from that data we will be able to determine the maximum torque force the brake can withstand.

Any Assumptions Involved in the Test

The main assumptions are that the calibration of the load is the same, and that the force produced by the user in this test is strictly tangential to the SDOF path.

Accepted Criteria

For our design to meet the requirements the brake must be able to resist a force of 25 N and torque of 11Nm

Test Results

The plot of these results of the full system force testing can be seen in Figure 11, in Appendix C. From the force testing of the bigger joint (1.75in bore size) we found that it could withstand a maximum of 14.811Nm of torque before the joint slid, which was greater than the expected value of 11Nm. However, it was noticeable that movement of the handle began to occur around this point. Observations of the movement showed that the shaft of the joint was not moving, but rather, the motion was caused by some looseness of the design. Some parts, such as the handle linkage and the keyway, were not completely coupled with each other, which was likely the source of the slack.

Evaluation

Results from the full system torque testing showed that the device successfully stops joint rotation from someone's hand when brakes are locked. However, there is some looseness of the handle that causes unwanted movement/slack.

3.2 The Motion of the SDOF Path Should Have Minimal Friction and Inertia

3.2.1 Measurement of SDOF Forces

This test involves measuring the torque from the handle when someone moves the devices along the SDOF path. This will assess how easily the user can move along the path.

Objectives

Assess the maximum force resistance when moving along an SDOF path with the handle.

Features Evaluated

The motion of the SDOF path and the measured torque on the handle

Test scope and Key Test Conditions

The motion from the joints that have 1.5in and 1.75in bore cylinders will be tested. The user will move the handle along the SDOF path back and forth several times while the cylinders are open.

Instruments and Test Setups Used

The load cell on the handle will measure the force, and the resulting torque on the joint will be computed. The measured moment arms from the handle to the 1.5in and 1.75in bore cylinders were 14.5in and 18in respectively.

Any Assumptions Involved in the Test

The main assumptions in this test is that the motion produced by the user is strictly tangential to the SDOF path.

Acceptance Criteria

Because it is difficult to objectively quantify what range of torque values allows the most comfortable or smooth path motion, we assessed the feedback from the person performing the test (Dr. Treadway) to get an idea if the motion was smooth overall or not, and used the corresponding data to see what torque values may have been the result of that response.

Test Results

The motion of the path, as described by Dr. Treadway, was fairly smooth and had minimal inertia. As shown in Figure 12 in Appendix C, the maximum measured torque value was approximately 2Nm, which may show that values below this threshold allows for easy motion.

Evaluation

The test results showed that the device was satisfactory in terms of the smoothness of the SDOF paths. This allows the device to have satisfactory ergonomic motion when a user operates it.

3.3 Measurement of Position from Rotary Encoder

Under each brake is a rotary encoder. These encoders measure the ‘counts’ of rotation, which can then be translated to degrees. Two tests were performed: one analyzing how accurately rotation can be measured using one break, and another testing how the angle measurements from multiple breaks can be combined to find handle position.

3.3.1 Single Encoder Test

In order to measure the angle that the link holds, a rotary encoder has been attached to each brake. The team used MATLAB simulink to verify that the angle positions are able to be read by the encoder, and that they are correct.

Objectives

Verify that the angle positions are able to read the encoder accurately

Features evaluated

The quality of the encoder data received, notably the accuracy and reliability of the values.

Test scope and Key Test Conditions

The test involved the use of only one encoder, connected to a shaft and fixed to a flat steady surface. The voltage values from the encoder will be measured. For this test, the encoder tested a single link system. Then the team used the moving link, and moved it a specified distance by hand. This movement was recorded by the encoder. The data of the encoder was then compared to the actual movement to determine the accuracy of the measurement.

Instruments and/or test setups used

The encoder was connected to the computer that is running MATLAB SIMULINK. By using a protractor, the team was able to apply a specific motion to the shaft, at a set degree angle.

Any Assumptions Involved in the Test

No major assumptions were made in this test.

Acceptance Criteria

For our project, accuracy within 5% of the angle is necessary. We picked this error range because it would prevent the accuracy of the overall handle location from becoming drastically affected.

Test Results

This test was successfully performed on the single linkage arm that we created. Through the use of MATLAB, and the E3 encoder from USAdigital, we were able to measure the movement of the linkage. We tested the position of the arm at three different points. From a reference point, designated as 0, we tested the positions at 90 degrees, 180 degrees, and 270 degrees. Since this is a 1800 CPR encoder, there should be 7200 total counts around the disc, because it is a quadrature encoder. When divided by 360, the number of counts per degree should be 20. At each of the points measured, the value of the counts at each point was well within the 5% error that was allowed. This test illustrates the accuracy of the encoders. The data retrieved from these tests can be found in Table 7.

Evaluation

This test proved that the encoder could successfully be used to find the angle that each brake was rotated to. All of the results fell within the expected error. The encoder reliability allowed us to proceed with the following test.

3.3.2 Measurement of Position from Rotary Encoder

The team will use MATLAB simulink to test the written code for the handle position, utilizing multiple encoders' data to calculate it.

Objectives

Verified that:

1. SIMULINK analyzes all 6 encoder values.
2. The code written to interpret the handle position operates correctly

Features evaluated

This test evaluated the ability to correctly measure the handle position using the written SIMULINK code.

Test scope and Key Test Conditions

The test utilized three brakes (and encoders) set at three different handle positions, and measured the angles that brakes at each of the given handle positions (A, B, and C). The MATLAB code calculated the perceived handle position at each of the positions.

Instruments and/or Test Setups Used

By connecting encoders with links, the handle can be moved and an SDOF path can be created. By marking the original point, and traveling to multiple spots of known distance, we were able to compare the encoder values of the starting and stopping positions with the actual values. The data from each encoder was read using simulink, and the data was run through the code. The X and Y positions of the handle were analyzed in the code.

Any Assumptions Involved in the Test

There were no major assumptions made in this test.

Acceptance Criteria

An acceptable result for the position measurement is within half of an inch in both the X and Y directions from the actual position.

Test Result

At each of the measured positions, at least one of the two trials had X and Y calculated positions that were within half an inch of the actual position of the handle. Only for a few trials did value differentials exceed that amount. However, being that the surface area of the target position markers were nonzero, which introduces error to the (x,y) position showed allows for a greater tolerance for error, and therefore these slight differentials are not cause for concern. Full test results for this evaluation can be found in Tables 4, 5, and 6.

Evaluation

The test was successful. The success of this test proves that this method can be applied to the full six link system. The encoders will not only be able read a single joint angle, but be able to successfully locate and track the position of the handle, which satisfies the requirement.

3.4 The Device Must Have A Minimum Trajectory Angle of 90 Degrees Over a 5x5in Area

3.4.1 Angle Constraint Test

This test verified the angle requirement between the paths created by each joint.

Objectives

The team used a matlab simulation to determine the path of the handle when the full linkage is assembled, graphing the SDOF path changes to verify that the angles are less than 90 degrees.

Features evaluated

The test evaluated the angle change between the different paths

Test scope & Key Test Conditions

This test was performed by graphing a path for each linkage from the beginning handle position.

Instruments and/or Test Setups Used

This test utilizes the MATLAB code used for judging the position of the handle, however the inputs are changed. Rather than being fed by the encoder, they are set to a nominal value of 150 degrees (except brake 6, which is set to 60 degrees). The path of each joint was graphed separately, showing a movement of 10 degrees in either direction of the set angle. These plots were overlaid to show the differences.

Acceptance criteria

For our test, the angle of the path change must be less than 90 degrees. This is because an angle that is above 90 degrees will cause the arm to perform an unnatural motion. This motion will disrupt the fluidity of the path, and will be strange for the tester.

Test Results

The test for the angle requirement was shown to be successful. The difference between the paths all had angles that were less than 90 degrees. The plotted graph can be in appendix E, Figure 15. This graph shows each of the plotted paths from the centerpoint.

Evaluation

The design fulfills the angle requirement, not surpassing 90 degrees between any adjacent paths.

3.4 Workspace size

Evaluation

The full workspace of the handle paths was initially estimated to be at least 12 inches in the Y direction and 5 inches in the X directions. After fully graphing the workspaces using the Matlab handle position code, the true workspaces was found to be approximately 11 inches in the X direction and 15 inches in the Y direction. This larger workspace is beneficial as it provides a larger area for the operator to create different paths. The graph of the workspace can be found in appendix E, Figure 14.

3.5 Ergonomics - The device should have a handle that can be easily gripped by a user who sits at a table

Evaluation

From the torque testing that we conducted for the single joint as well as for the full assembly, it was proven that the metal handle could be easily gripped by a user who sits at a table.

3.6 Safety Requirements & ISO/IRB

Evaluation

While the pneumatic cylinders at the joints may act as hazardous pinching points in the process of extending or retracting them, the device is successfully designed such that the user operating it is far away from these parts. Additionally, in the process of testing, it was agreed that the haptic system also satisfies all four clauses (5.10.2 - 5.10.5) by the ISO 10218, ISO/TS 15066 standard for collaborative robots. These can be found from [4]. Lastly, the device did not show any representation of being physically invasive or painful, which satisfies the Federal Guidelines from the Institutional Review Board

3.7 Software used to control the system should be well documented.

Evaluation

The equations found in Appendix F, Tables 2 and 3, represent the equations utilized in the MATLAB code. Any tests done used these equations, with slightly varied inputs, to measure paths and handle position. Full code can be found in Appendix G.

3.8 A minimum of 6 SDOF paths are required.

Evaluation

In order to create a minimum of 6 SDOF paths we designed a system of 6 brakes that would switch on and off to create these different paths. Although due to our current limitations as discussed in our updated project proposal we can only present 5 of the 6 physical brakes. However, once the final brake is completely machined and assembled the physical prototype will have 6 SDOF paths.

4. Conclusion

The final prototype of our design does accomplish what we promised in our most recent project plan. In addition, the design achieves all of the project requirements stated in the updated project proposal. However, we noticed that there was slack in the linkage assembly because the handle, linkage and the keyway were not completely coupled with each other. To fix this problem we could include ball transfers under the handle and redesign the connection between the small shaft and the clamp to be more solid. In addition, the encoder was very challenging and time consuming to mount. One solution to this problem is to extend the length of the keyway shaft to provide additional room to ease the struggle of mounting the encoder. In terms of additional testing, it would be beneficial to conduct more force/torque testing once adjustments have been made for the slack issue. By performing additional force testing it would provide insight as to whether the slack has been addressed sufficiently or if more adjustments need to be made.

Appendix A: Setup, Operating and Safety Information

Setup, Operating and Safety Instructions:

Before turning on the pressure to the cylinders, be sure that the regulators are fully closed, as this will prevent any initial sudden movement of the pneumatic cylinders. Make sure that the regulator reads about 70-75psi, which is the maximum possible pressure from the supply.

The operation of a single valve requires the following circuit in Figure 8 in Appendix B, where the input voltage, Vin is the signal from the data acquisition system, and the output voltage, Vout, goes to the leads of the valve. If a user plans on testing all six SDOF paths, be sure that six of these circuits are built for each valve to operate the corresponding cylinders.

Safety of Physical Operating:

Because the pneumatic cylinder heads rapidly open and close with significant pressure, be sure to keep your hands and person away from them at all times of operating, especially when someone uses the MATLAB Simulink code to operate the data acquisition system.

Operating the Encoder:

The covering of the encoder is optional, however it is recommended. If the encoder is scratched or moved by outside forces, it will not be able to read the data. It is important when using the encoder, to correctly input the wires into the encoder, and insert the opposite end of the wire into the corresponding computer ports. If any of the 5 wires are input incorrectly it will not read the data. When reading the encoders in Matlab, the rotary counts can be evaluated in a scope. Each encoder will be evaluated in a separate scope.

Appendix B: Valve Information

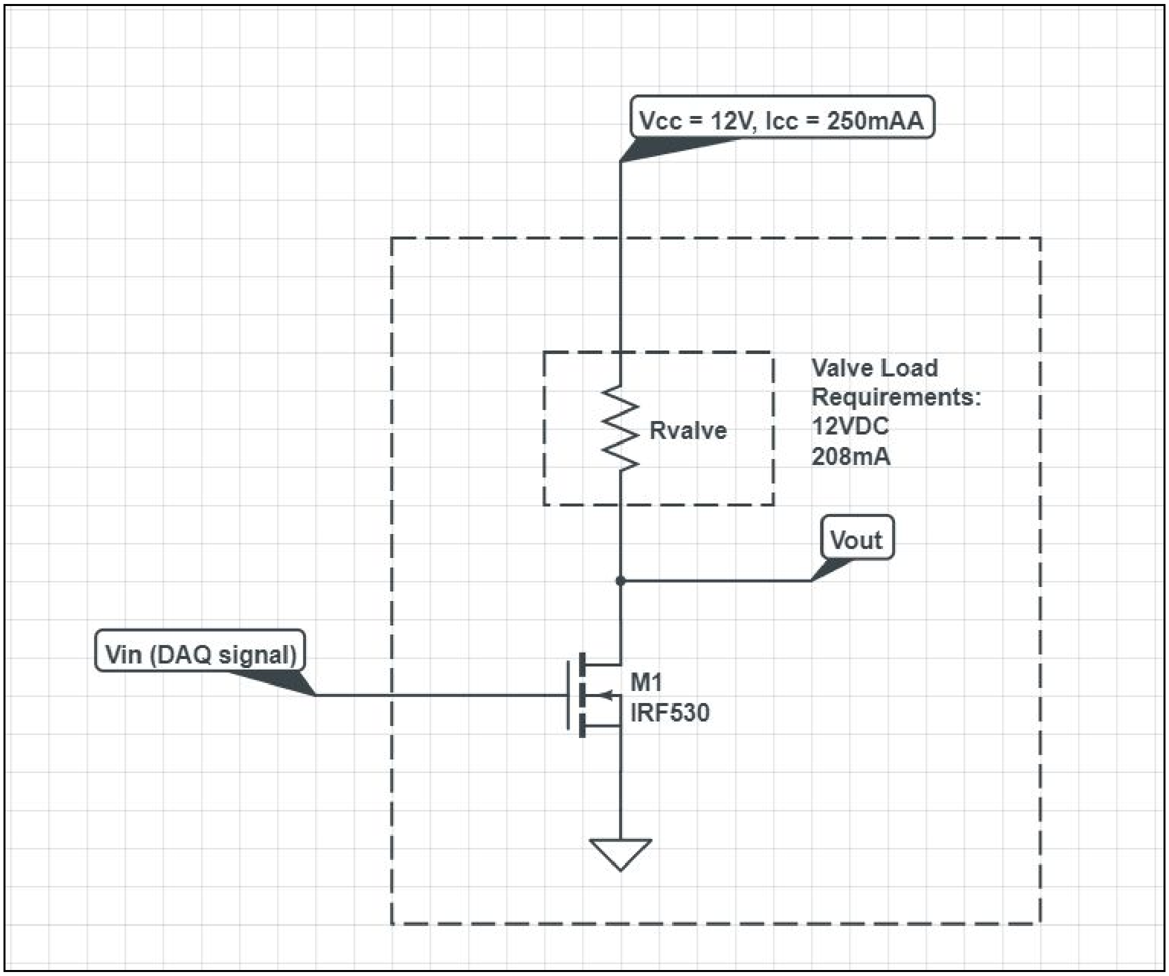

Figure 8. Circuit Schematic for Valve. Note that Vin is the data acquisition signal, and the valve activates (opens) when Vin=5V and closes when Vin=0V. The power supply has

Appendix C: Torque Testing Information

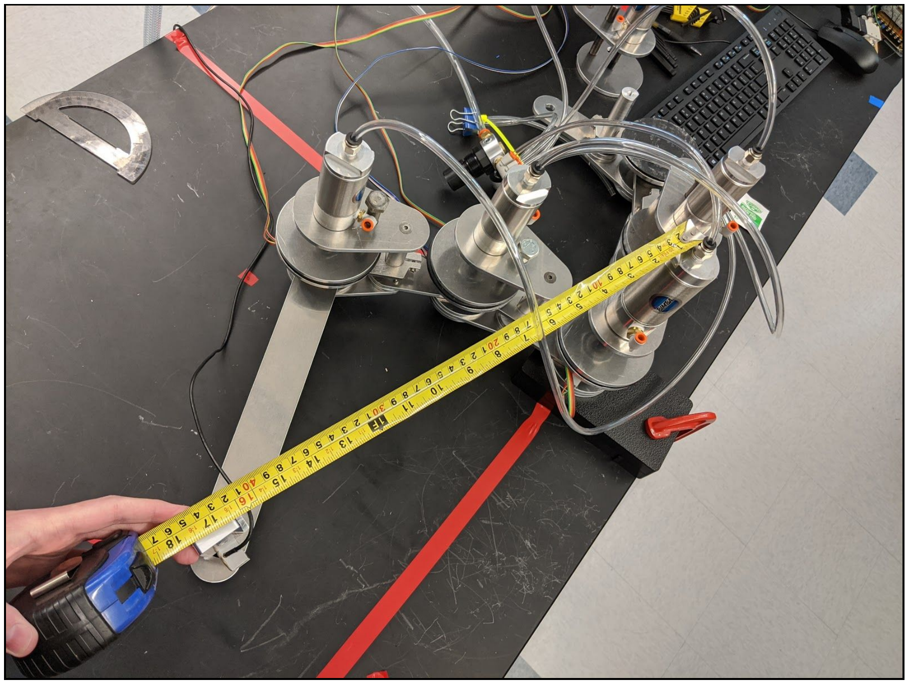

Figure 9. Force Testing Setup for Full System Length

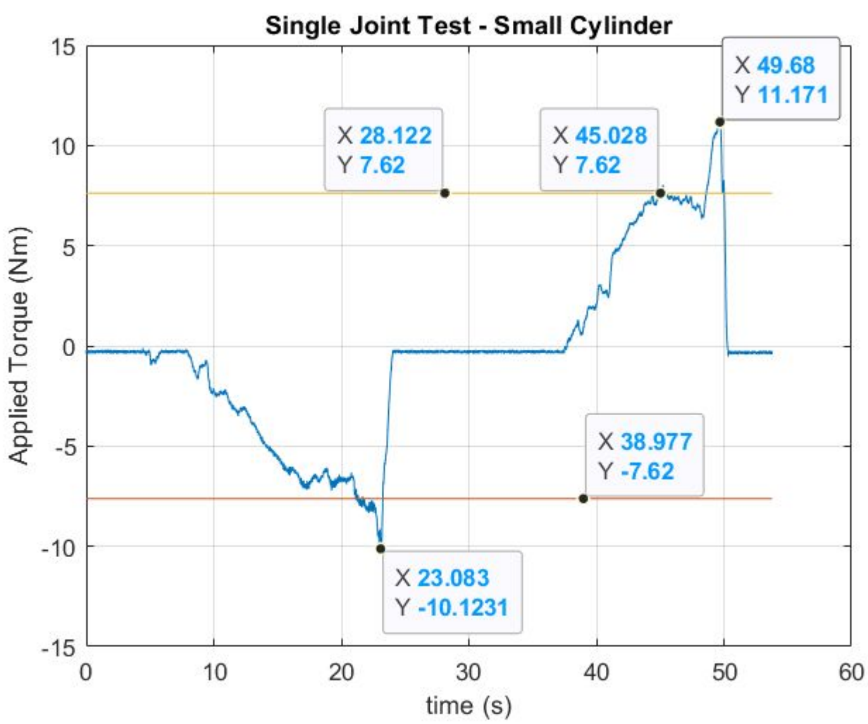

Figure 10. Torque results of a single joint with a bore size of 1.5in (small). The red line is the expected torque that the joint should resist

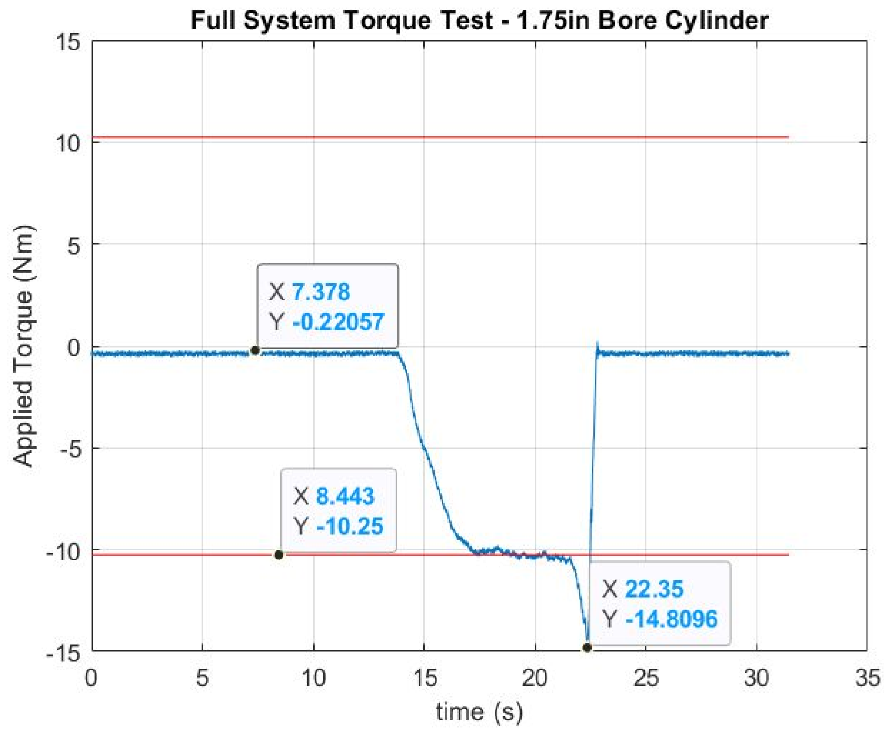

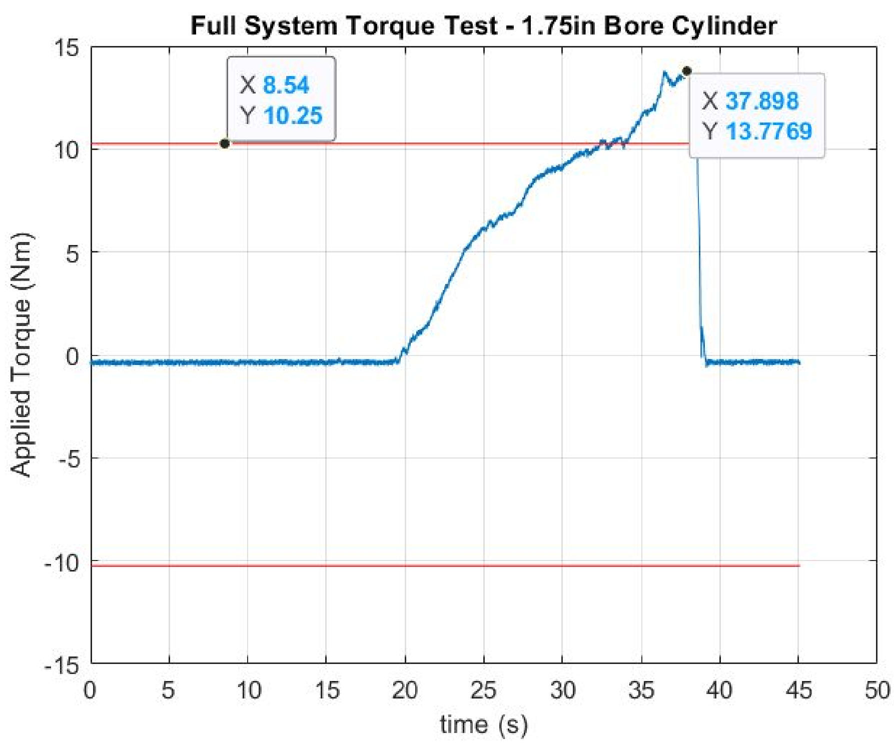

Figure 11. Torque results for full system length (17.4in) testing for turning CW (Top) and CCW (Bottom). The red lines are the expected torques that the joints should handle.

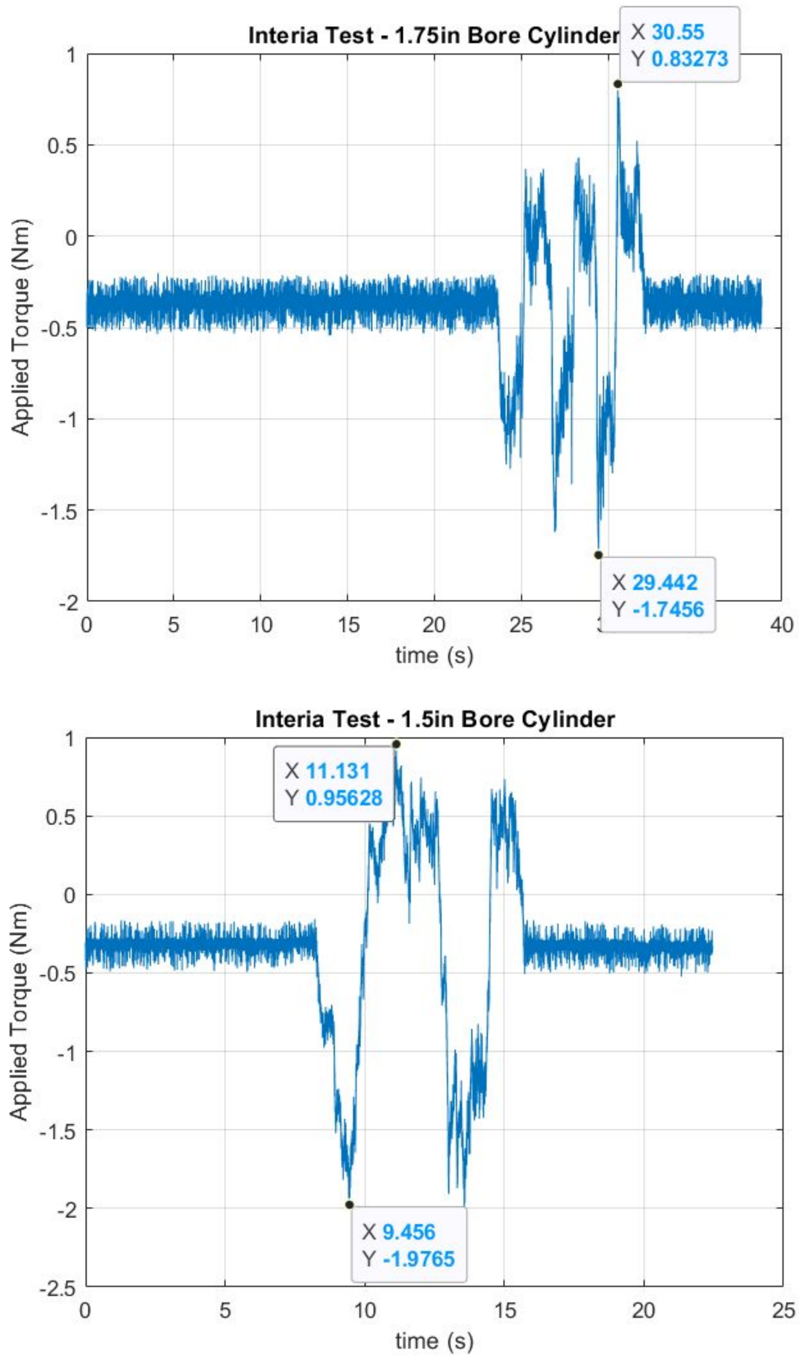

Figure 12. Torque measurements obtained from moving along the SDOF path.

Appendix D: Model Parameters for SDOF Simulations

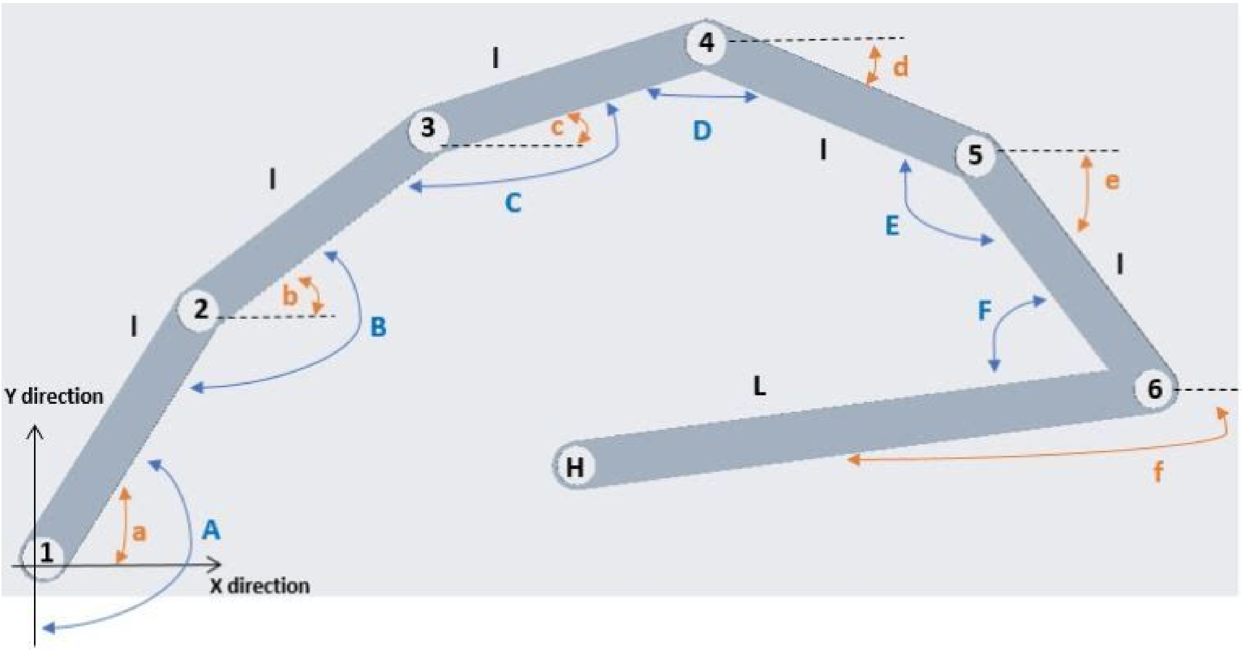

Figure 13. Aerial view of the linkage system, showing the measured angles (Blue) and the active angle (Orange) used for the calculations of handle position

Appendix E: Matlab Simulations

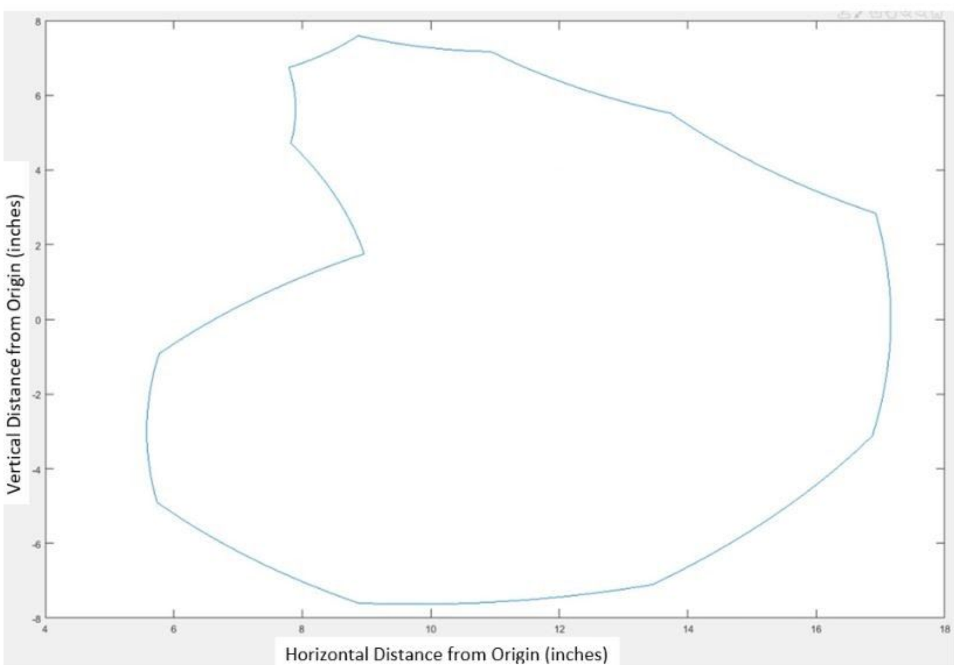

Figure 14. Shows the complete workspace of the handle position, displaying the X and Y distances from the origin, as the device fully contracts and expands

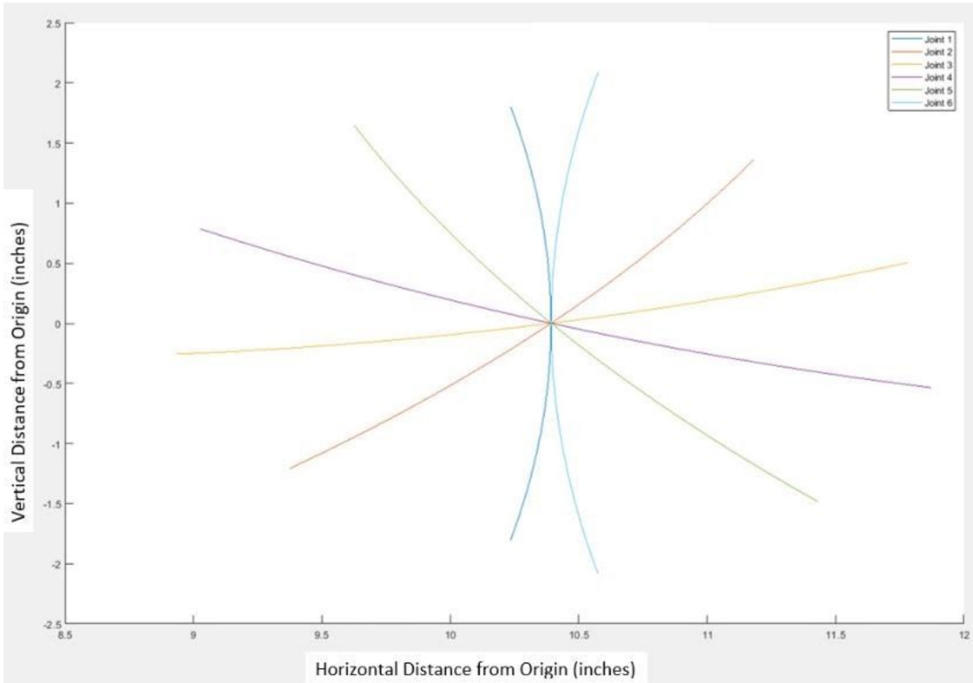

Figure 15. Shows the 6 different SDOF paths created by the 6 brakes in the link. Starting from the center point, the handle could take any path, depending on the brake.

Appendix F: Tables

Table 1. Maximum radius and torques applied at each brake

Joint/ Cylinder	Maximum Radius in-(m)	Maximum Force (N)	Maximum Torque (Nm)
1	17.38 - (0.44)	25	11.00
2	15.13 - (0.38)	25	9.50
3	13.26 - (0.34)	25	8.50
4	11.91 - (0.30)	25	7.50
5	11.43 - (0.29)	25	7.25
6	12.00 - (0.30)	25	7.50

Table 2. The brakes from Figure 2, showing the encoder data, and the corresponding angle equations used to analyze the location.

Brake	Measured Angle	Active Angle
1	A	a = A - 90
2	B	b = B + a - 180
3	C	c = C + b - 180
4	D	d = D + c - 180
5	E	e = E + d - 180
6	F	f = F + e -180

Table 3. Equations used to find the X and Y direction of the handle based on the active angles shown in Table 2

Direction	Equation
X direction	X = l*[cos(a) + cos(b) + cos(c) + cos(d) + cos(e)] + L*cos(f)
Y direction	Y = l*[sin(a) + sin(b) + sin(c) + sin(d) + sin(e)] + L*sin(f)

Table 4. Raw encoder data counts (and corresponding degree angle) for each brake, when the handle is at the first test point, and the corresponding calculated position

	Encoder 1 (Counts)	Angle 1 (degrees)	Encoder 2 (Counts)	Angle 2 (degrees)	Encoder 3 (Counts)	Angle 3 (degrees)	Nominal Position (X in, Y in)	Calculated Position (X in, Yin)
Trial 1	1599	80.0	1086	54.3	187	9.4	(14.1, -1.5)	(13.5, -1.1)
Trial 2	1531	76.6	1165	58.3	133	6.7		(13.6, -0.9)

Table 5. Raw encoder data counts (and corresponding degree angle) for each brake, when the handle is at the second test point, and the corresponding calculated position

	Encoder 1 (Counts)	Angle 1 (degrees)	Encoder 2 (Counts)	Angle 2 (degrees)	Encoder 3 (Counts)	Angle 3 (degrees)	Nominal Position (X in, Y in)	Calculated Position (X in, Yin)
Trial 1	1815	90.8	530	26.5	-791	-39.6	(6.5, 13.0)	(6.5, 13.0)

Trial 2	1862	93.1	502	25.1	-826	-41.31		(6.1, 13.0)

Table 6. Raw encoder data counts (and corresponding degree angle) for each brake, when the handle is at the third test point, and the corresponding calculated position

	Encoder 1 (Counts)	Angle 1 (degrees)	Encoder 2 (Counts)	Angle 2 (degrees)	Encoder 3 (Counts)	Angle 3 (degrees)	Nominal Position (X in, Y in)	Calculated Position (X in, Yin)
Trial 1	1112	55.6	573	28.7	251	12.6	(17.3, 9.3)	(17.2, 8.9)
Trial 2	515	25.75	1369	68.45	-99	-5.0		(16.8, 8.8)

Table 7. Results from the single link encoder test

	Measured Values	Nominal Values	Percent Difference
90 Degrees	**1784**	**1800**	**0.88%**
180 Degrees	**3476**	**3600**	**3.44%**
270 Degrees	**5292**	**5400**	**2.0%**

Appendix G: Code

Position function:

```
function [X, Y] = Position(A,B,C,D,E,F,l,L)
 a = A - 90;
 b = B + a - 180;
 c = C + b - 180;
 d = D + c - 180;
 e = E + d - 180;
 f = F + e - 180;
 X = l*[cosd(a) + cosd(b) + cosd(c) + cosd(d) + cosd(e)] + L*cosd(f);
 Y = l*[sind(a) + sind(b) + sind(c) + sind(d) + sind(e)] + L*sind(f);
end
```

Plotting workspace and path angles

```
Ax = 160
Bx = 160
Cx = 160
Dx = 160
```

```
Ex = 160
Fx = 70

A = 150
B = 150
C = 150
D = 150
E = 150
F = 60

An = 140
Bn = 140
Cn = 140
Dn = 140
En = 140
Fn = 50

Ae = 140:160
Be = 140:160
Ce = 140:160
De = 140:160
Ee = 140:160
Fe = 50:70

Ar = 160:-1:140
Br = 160:-1:140
Cr = 160:-1:140
Dr = 160:-1:140
Er = 160:-1:140
Fr = 70:-1:50

l = 6
L = 12
[X, Y] = Position(An,Bn,Cn,Dn,En,Fn,l,L)
```

```
[X1, Y1] = Position(An,Bn,Cn,Dn,En,Fe,I,L)
[X2, Y2] = Position(An,Bn,Cn,Dn,Ee,Fx,I,L)
[X3, Y3] = Position(An,Bn,Cn,De,Ex,Fx,I,L)
[X4, Y4] = Position(An,Bn,Ce,Dx,Ex,Fx,I,L)
[X5, Y5] = Position(An,Be,Cx,Dx,Ex,Fx,I,L)
[X6, Y6] = Position(Ae,Bx,Cx,Dx,Ex,Fx,I,L)

[X7, Y7] = Position(Ax,Bx,Cx,Dx,Ex,Fr,I,L)
[X8, Y8] = Position(Ax,Bx,Cx,Dx,Er,Fn,I,L)
[X9, Y9] = Position(Ax,Bx,Cx,Dr,En,Fn,I,L)
[X10, Y10] = Position(Ax,Bx,Cr,Dn,En,Fn,I,L)
[X11, Y11] = Position(Ax,Br,Cn,Dn,En,Fn,I,L)
[X12, Y12] = Position(Ar,Bn,Cn,Dn,En,Fn,I,L)

[X13, Y13] = Position(A,B,C,D,E,Fe,I,L)
[X14, Y14] = Position(A,B,C,D,Ee,F,I,L)
[X15, Y15] = Position(A,B,C,De,E,F,I,L)
[X16, Y16] = Position(A,B,Ce,D,E,F,I,L)
[X17, Y17] = Position(A,Be,C,D,E,F,I,L)
[X18, Y18] = Position(Ae,B,C,D,E,F,I,L)

plot ([X1,X2,X3,X4,X5,X6,X7,X8,X9,X10,X11,X12],[Y1,Y2,Y3,Y4,Y5,Y6,Y7,Y8,Y9,Y10,Y11,Y12])

Hold on
Plot (X13,Y13)
Hold on
Plot (X14,Y14)
Hold on
Plot (X15,Y15)
Hold on
Plot (X16,Y16)
Hold on
Plot (X17,Y17)
Hold on
```

Plot (X18,Y18)

Bibliography (IEEE)

[1] E. Treadway, Z. Gan, C. D. Remy, and R. B. Gillespie, “Toward Controllable Hydraulic Coupling of
Joints in a Wearable Robot,” IEEE Trans. Robot., vol. 34, no. 3, pp. 748–763, 2018.

[2] M. R. Reed and W. J. Book, “Modeling and control of an improved dissipative passive haptic display,”in IEEE International Conference on Robotics and Automation, April 2004, pp. 311–318.

[3] United States Government, 2017. Federal Policy for the Protection of Human Subject. Retrieved September 23, 2019 from: https://www.federalregister.gov/documents/2017/01/19/2017-01058/federal-policy-for-the-protection-of-human-subjects#p-1366

[4] Bjorn, M., 2015. “New safety standards for collaborative robots ABB YuMi dual-arm robot: Workshop IROS 2015 - Robotic co-workers - methods, challenges, and industrial test cases.” ABB Corporate Research. Retrieved September 23, 2019 from: https://www.researchgate.net/publication/282778835_New_safety_standards_for_collaborative_robots_ABB_YuMiR_dual-arm_robot

[5] J. Moore et al. 2011. Disc Friction: Mechanics Map. Retrieved May 5, 2020 from http://adaptivemap.ma.psu.edu/websites/6_friction/disc_friction/discfriction.html

Signatures		
Project Name: Passive Haptic Device for Virtual Environments		
The undersigned have reviewed and approved the final version of this document.		
	Date Received	**Date Approved**
Team Members: **Lydia Matteson-***Lydia S Matteson* **Morgan Jones -***Morgan R. Jones*	**/2020** **/2020**	**/2020** **/2020** **/2020**

Sam Hinojosa - *Samuel D. Hinojosa*	**/2020**	
Team Adviser: *Emma Treadway*	**3/31/2020**	**3/31/2020**

Document Change Control **This section records the revisions to this document.**		
Version Number	**Date of Issue**	**Brief Description of Change**